High-Pressure—High-Temperature Polymorphism in Ta: Resolving an Ongoing Experimental Controversy

L. Burakovsky,[1] S. P. Chen,[1] D. L. Preston,[2] A. B. Belonoshko,[3] A. Rosengren,[3] A. S. Mikhaylushkin,[4] S. I. Simak,[4] and J. A. Moriarty[5]

[1]*Theoretical Division, Los Alamos National Laboratory, Los Alamos, New Mexico 87545, USA*
[2]*Physics Divisions, Los Alamos National Laboratory, Los Alamos, New Mexico 87545, USA*
[3]*Institute of Theoretical Physics, AlbaNova University Center, Royal Institute of Technology, SE-10691 Stockholm, Sweden*
[4]*Department of Physics, Chemistry and Biology (IFM), Linköping University, SE-58183 Linköping, Sweden*
[5]*Condensed Matter and Materials Division, Lawrence Livermore National Laboratory, Livermore, California 94551-0808, USA*

(Received 2 April 2010; published 21 June 2010)

Phase diagrams of refractory metals remain essentially unknown. Moreover, there is an ongoing controversy over the high-pressure melting temperatures of these metals: results of diamond anvil cell (DAC) and shock wave experiments differ by at least a factor of 2. From an extensive *ab initio* study on tantalum we discovered that the body-centered cubic phase, its physical phase at ambient conditions, transforms to another solid phase, possibly hexagonal omega phase, at high temperature. Hence the sample motion observed in DAC experiments is very likely not due to melting but internal stresses accompanying a solid-solid transformation, and thermal stresses associated with laser heating.

DOI: 10.1103/PhysRevLett.104.255702 PACS numbers: 81.30.−t, 64.70.D−, 64.70.K−, 71.15.Pd

There is an ongoing controversy over the high-pressure melting of groups V and VI refractory metals that began with the first diamond anvil cell (DAC) measurements of the melting temperatures of V, Ta, Cr, Mo, and W nearly a decade ago [1]. In the DAC experiments, melting at a given pressure, P, is assumed to coincide with the onset of sample surface motion as the temperature, T, is raised by laser heating of the sample. Melting temperatures, T_m, as determined by this technique, are consistently lower than those obtained from shock wave (SW) experiments, wherein T_m is determined from a calculated equation of state (EOS) using the measured P and density, ρ, at which the longitudinal sound speed in the equilibrium shock state (Hugoniot) suddenly drops with increasing P because of the loss of shear strength on melting. The discrepancy between the DAC and SW values of T_m at high P is at least a factor of 2: for V at ~225 GPa, $T_m \sim 3000$ K from the extrapolated DAC melt curve [1], as compared with a SW value of ~7800 K [2]; for Ta at ~300 GPa, an extrapolated DAC [1,3] $T_m \sim 4000$ K versus a SW [4] ~10000 K; and for Mo at $P \sim 400$ GPa, an extrapolated DAC [1,5] $T_m \sim 4000$ K versus a SW [6] ~10000 K.

The refractory metals have a characteristic body-centered cubic (bcc) structure under ambient conditions, and consequently, all but one of the theoretical efforts to resolve this DAC/SW melting controversy have been based on comparisons of bcc melt curves [7]. The exception is our previous work on Mo [7,8], where we considered other solid phases. Using *ab initio* density functional theory (DFT) methods, we found that the face-centered cubic (fcc) structure melts at a higher T and is hence more stable than bcc at Ps exceeding roughly 150 GPa. This does not prove that the fcc structure is the most stable phase there, only that it is more stable than bcc; indeed, there is evidence [8] that other crystal structures may be more stable than fcc at high P-T, and therefore may melt at even higher Ts than fcc. In any case, our calculated fcc melt curve is consistent with the high observed SW T_m of Mo, and moreover, our estimated bcc-fcc phase boundary at low P is consistent with the DAC melt curve, as well as with the observed break in the Hugoniot sound-speed curve at ~200 GPa prior to shock melting [6]. On that basis, we proposed [7] that the buildup of internal nonhydrostatic stresses accompanying a solid-solid (SS) phase transformation is responsible for the observed material flow of Mo at high P-T in the DAC experiments. Such an explanation could also apply to the other refractory metals.

In addition to sample surface flow, the disappearance of *some* bcc x-ray diffraction lines at the DAC T_ms in subsequent experiments on Ta [3] and Mo [5] contributed to the conclusion that melting had occurred. However, the inverse problem of deducing structure from diffraction patterns is nontrivial, and can easily lead to erroneous conclusions. Indeed, the claimed discovery of a new phase of Zr, namely, Zr glass [9], in the vicinity of the bcc to hexagonal omega (hex-ω) phase transition boundary was later retracted [10]. The initial conclusion was based on the disappearance of *some* solidlike x-ray diffraction lines, but a subsequent more careful analysis revealed that the disappearance of the lines occurred because of rapid crystal growth at Ts above the phase transformation. Similarly, rapid recrystallization, or the growth of a new crystal phase, can occur in DAC melting experiments under the P-T conditions close to those of a SS transition. In particular, in their analysis of the DAC experiments on Mo [11], Ross *et al.* observed permanent rapid recrystallization of the sample "with a dramatic change of the Bragg peak intensity, from one solidlike diffraction pattern to the next,

probably due to locally preferred orientation nucleation during recrystallization;'' here ''the next'' solidlike pattern must be that of an ingrowing phase more stable than bcc.

A recent study by Wu *et al.* [12], motivated in part by the possibility that shear stresses play a key role in the structural transformations occurring in the DAC, performed molecular dynamics (MD) simulations of Ta with a quantum-based, multi-ion MGPT (model generalized pseudopotential theory) interatomic potential [13]. They found a shear-induced transformation from bcc to a partially disordered, partially crystalline structure, and the P-T dependence of the transformation coincides closely with the DAC melt curve. They interpreted this transformation as a Bingham-like plastic flow, where the shear-dependent flow character is linked to a flat energy landscape associated with the geometric distortion of {110} planes, and as such, it is likely tied to high P-T polymorphism. In this regard, previous MGPT studies at high P-T conditions in Ta have shown both a substantial elastic softening of the bcc structure [14], which is presumably a precursor to any phase transition in the solid, and the appearance of a mechanically stable and energetically competitive cubic $A15$ phase [15]. Moreover, as discussed below, we have carried out both *ab initio* and MGPT MD simulations of high P Ta melting from different phases, and each predicts the existence of a solid phase more stable than bcc at high P-T.

We now turn to our present *ab initio* study of Ta, which conclusively demonstrates that Ta is polymorphic at high P-T. Our DFT calculations of the electron and phonon spectra, as well as our *ab initio* MD simulations of Ta, were performed in the framework of the frozen-core all-electron projector augmented wave method [16], as implemented in the program VASP [17]. The phonon calculations were carried out in the framework of the supercell approach (see [18] for details). To maintain high accuracy we used $3 \times 3 \times 3$ supercells. The energy cutoff was set to 400 eV. Exchange and correlation effects were treated within the generalized gradient approximation (GGA) [19]. The semicore $4p$ states of Ta were treated as valence. The integration over the Brillouin zone was based on the Monkhorst-Pack scheme [20]. Relaxation of the structural parameters (e.g., c/a ratios for the hcp, dhcp, and hex-ω phases) and force calculations were carried out according to the Methfessel-Paxton scheme [21], while total-energy calculations were performed using the tetrahedron method with Blöchl corrections [22].

In Fig. 1 we compare the $T = 0$ K EOS for bcc-Ta given by VASP, using both local density approximation (LDA) and GGA implementations of DFT, to the $T = 300$ K experimental one. As seen in Fig. 1, the experimental data points are bracketed by the two VASP curves, which demonstrates the validity of our computational framework.

The calculations at $T = 0$ K (Fig. 2) show that bcc is the lowest-energy solid structure over the entire P range considered, 0–1 T Pa. The c/a ratio of the hex-ω phase of Ta as a function of P is shown in the inset of Fig. 2. It is seen

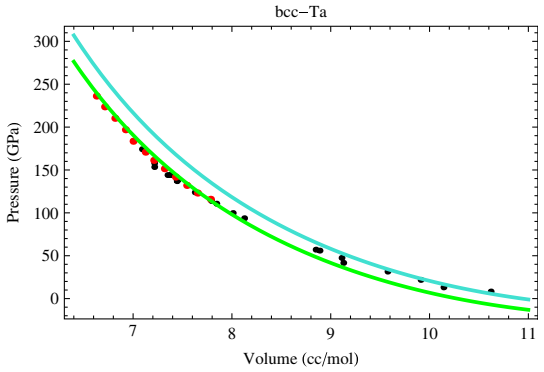

FIG. 1 (color online). EOS for bcc-Ta: $T = 0$ K VASP with LDA (green [light gray] curve) and GGA (turquoise [medium gray] curve) vs the $T = 300$ K experimental data points of Refs. [30] (black) and [31] (red [dark gray]).

that, with increasing P, it tends to the ''ideal'' bcc value of $\sqrt{3/8} \approx 0.6124$. Interestingly, the bcc phase is the only mechanically stable phase among all those considered up to 1 T Pa. The $T = 0$ K phonon spectra of the other phases contain imaginary frequencies at all Ps considered. With increasing P, the mechanical instability of each of these phases is enhanced, which is in accord with the overall increase in the total energy differences with P, but at sufficiently high T, these phases become mechanically stable, due to a combination of ion-thermal and electron-thermal effects, and hence thermodynamically they are either stable or metastable.

We next performed a suite of finite T *ab initio* MD simulations of melting from the bcc, fcc, hcp, dhcp, $A15$, and hex-ω phases of Ta using the so-called Z method [23]. The system sizes, simulation times, etc., were the same as those used in our previous simulations of Mo melting [7].

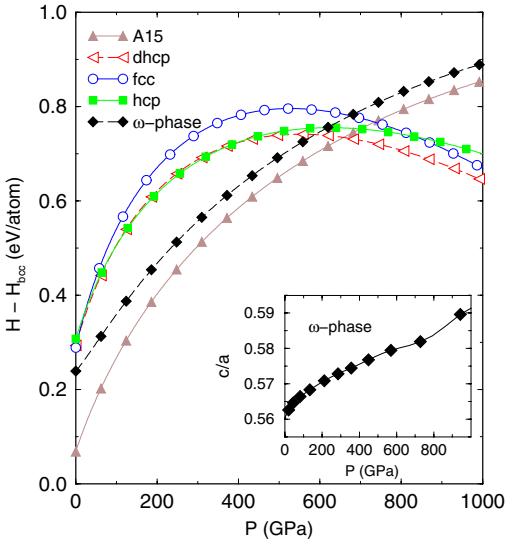

FIG. 2 (color online). Pressure dependence of the $T = 0$ K enthalpies of the fcc, hcp, dhcp, $A15$, and hex-ω structures of Ta relative to the $T = 0$ K enthalpy of the bcc phase; pressure dependence of c/a ratio for the hex-ω phase at $T = 0$ K (inset).

We find that all of the solid phases considered in Ta become mechanically stable at high T. They all have normal melt curves (solid-liquid coexistence lines), three of which are shown in Fig. 3, along with the experimental DAC data [3], and our estimated shock Hugoniot. Not shown are: $A15$ which is indistinguishable from bcc within the error bars, fcc which is close to hcp, and dhcp which is the lowest curve of all. For the sake of clarity, the Z isochores from which the melt curves are determined are not shown in Fig. 3, although they are typical and similar to those seen in Fig. 4. Our bcc melt curve is close to the previous *ab initio* result of Ref. [24] and about 20% lower at 500 GPa than the result of the MGPT MD simulations presented below, which do not include electron-thermal contributions.

In Fig. 3, only the hex-ω melt curve crosses the bcc one—the intersection point is at ~70 GPa and 5650 K; hence, the hex-ω phase of Ta is more stable than bcc at higher Ps.

With regards to the bcc-hex-ω phase boundary in Ta, we have used the Clausius-Clapeyron formula to estimate its slope near the bcc—hex-ω—liquid triple point: $-(100–120)$ K/GPa. If approximated by a straight line, this phase boundary would cross the Hugoniot at ~100 GPa and 2400–2500 K (see Fig. 3); below we compare this prediction with Hugoniot sound speed data. The shock melting point, that is, the intersection of the Hugoniot and the hex-ω melt curve, is at $(P, T) \sim$ (300 GPa, 11500 K). Our calculated T_m is thus about 15% higher than the original SW estimate of 10 000 K [4].

In addition to our *ab initio* simulations of the high P-T solid phases of Ta, we also carried out a series of MGPT MD simulations of the bcc, fcc, and $A15$ phases of Ta using the Z method. Our goal was to check if there exists another solid phase more stable than bcc, and that the shear-dependent flow character in the MGPT MD simulations on bcc Ta by Wu *et al.* [12] can be explained as being associated with a phase transformation from bcc to that phase on increasing T. The calculations were carried out at a number of volumes from 23 Å^3/atom ($P \sim -30$ GPa at $T = 0$ K) down to 10 Å^3/atom ($P \sim 350$ GPa at $T = 0$ K). We used a 250-atom bcc supercell obtained by $5 \times 5 \times 5$ multiplication of a 2-atom unit cell, a 256-atom fcc supercell ($4 \times 4 \times 4$, 4-atom unit cell), and a 216-atom $A15$ supercell ($3 \times 3 \times 3$, 8-atom unit cell). The time step was 1 fs to minimize numerical errors. The system was equilibrated for 8000 time steps, after which the averages were accumulated. All MGPT results for Ta, either presented or cited, were calculated with version 4.0 of the MGPT potential (also known as Ta4 or Ta-IV), also used by Wu *et al.* [12]. In Fig. 4, we show three pairs of bcc-fcc Z isochores (16, 12, and 10 Å^3/atom) and one $A15$ Z isochore (10 Å^3/atom). To within the statistical errors, the high-P $A15$ and bcc Z isochores are indistinguishable, as is the case for their *ab initio* counterparts. The fact that the $A15$ and bcc melt curves are very close, which implies nearly equal free energies at high T, is consistent with the appearance of $A15$ during the intermediate stages of previous MGPT MD Ta solidification simulations [15]. The fcc phase is unquestionably more stable than bcc at high P-T. Based on accurate fits to the MD data using the Simon functional form, the bcc-fcc intersection occurs at about 15 GPa (and 4300 K).

We now show that our linearly extrapolated *ab initio* bcc-hex-ω phase boundary is in excellent agreement with Hugoniot sound speed data on Ta. The earliest data set consisted of 12 points, eleven of which were published [4]. The twelfth unplublished data point was recently provided to us [25]. With the addition of the data point from [26], and the three most recent data points from [27], Fig. 5 displays all available Ta Hugoniot sound speed data (ambient sound speeds, also included in Fig. 5, are given by

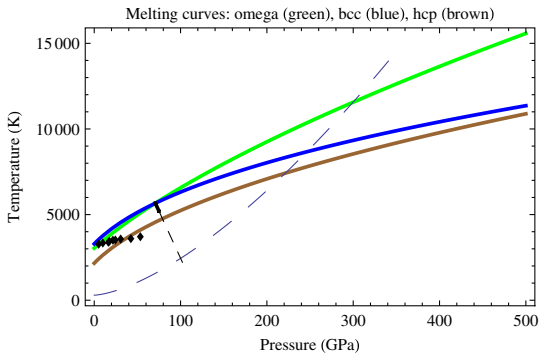

FIG. 3 (color online). *Ab initio* melt curves of the bcc (blue [medium gray]), hex-ω (green [light gray]), and hcp (brown [dark gray]) phases of Ta, along with the experimental data of Ref. [3] (black diamonds), our estimated shock Hugoniot (long dashed line), and our approximate bcc-hex-ω phase line (short dashed line).

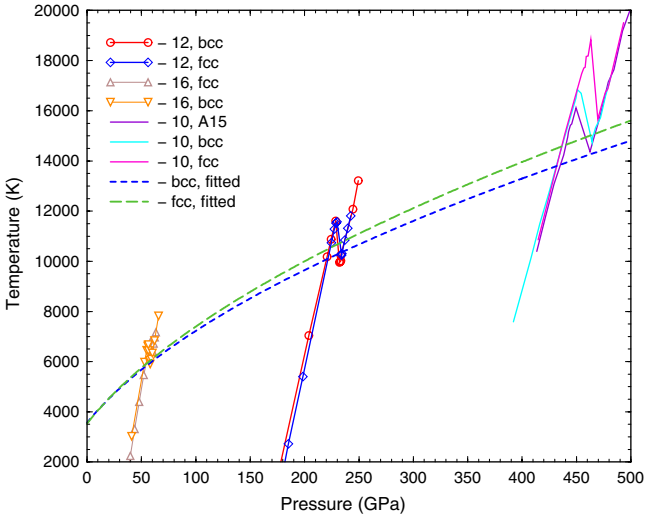

FIG. 4 (color online). Z isochores for bcc, fcc, and $A15$ Ta at volumes of 16, 12, and 10 Å^3/atom (shown as "16, bcc," "16, fcc,", etc.) obtained by MGPT MD. Dashed lines are our best fits to the bcc (blue [dark gray]) and fcc (green [light gray]) results.

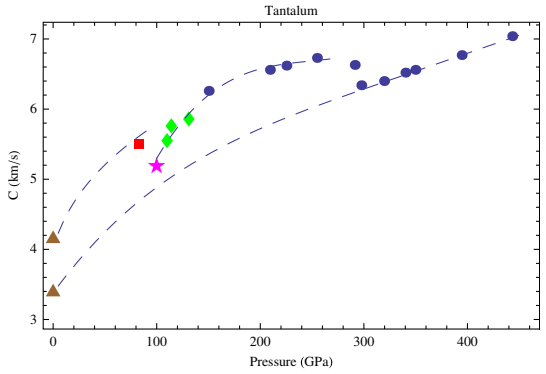

FIG. 5 (color online). Hugoniot sound speed data on Ta from Refs. [4] (blue circles), [25] (magenta star), [26] (red square), [27] (green diamonds), along with ambient values (brown triangles). Dashed lines are a guide to the eye only. However, the low-P upper segment and the whole lower line closely follow, respectively, $c_L \equiv \sqrt{(B + \frac{4}{3}G)/\rho}$ and $c_B \equiv \sqrt{B/\rho}$ for bcc-Ta [14].

$c_L = \sqrt{(B + 4/3G)/\rho}$ and $c_B = \sqrt{B/\rho}$ with ambient bulk modulus, B, shear modulus, G, and ρ from [28]). The discontinuity in c_L at ~100 GPa is very possibly the signature of a SS phase transformation. Remarkably, the intersection of our extrapolated bcc-hex-ω phase boundary and the estimated Hugoniot in Fig. 3 is also located at about 100 GPa.

The present investigation confirms that the bcc structure of Ta is supplanted by another solid phase at high Ps and Ts. Although our calculations on Ta do not rule out the possible existence of additional high P phases more stable than any considered in this study, the hex-ω phase of Ta predicted by our *ab initio* approach is a very likely candidate for the high P-T structure of Ta above ~70 GPa. We note that this phase was observed in a shock-recovered sample of Ta [29], although the material was shocked to only 45 GPa and ~550 K, where, according to Figs. 2 and 3, bcc is the stable phase. In any case, the discovered polymorphism in Ta makes a SS transformation from bcc to a higher T phase, possibly the hex-ω phase, a viable mechanism for the observed material flow in the DAC experiments. The flow occurs because of the rising internal stresses accompanying the SS transformation and the thermal stresses associated with laser heating.

Computations were performed using the facilities at the Swedish National Infrastructure for Computing (SNIC) and the LANL Coyote cluster. L. B., S. P. C., and D. L. P. wish to thank the U. S. Department of Energy (DOE) for financial support. A. B. B., A. R., A. S. M., and S. I. S. wish to thank the Swedish Research Council (VR) and the Swedish Foundation for Strategic Research (SSF) for financial support. A. S. M. acknowledges financial support from LINNEA center (Linköping). The work of J. A. M. was performed under the auspices of the U. S. DOE by Lawrence Livermore National Laboratory under Contract No. DE-AC52-07NA27344. We also wish to thank R. Hixson for giving us the unpublished sound speed data point by Brown and Shaner, and for very valuable comments and suggestions.

[1] D. Errandonea *et al.*, Phys. Rev. B **63**, 132104 (2001).
[2] C. Dai *et al.*, J. Phys. D **34**, 3064 (2001).
[3] D. Errandonea *et al.*, J. Phys. Condens. Matter **15**, 7635 (2003).
[4] J. M. Brown and J. W. Shaner, in *Shock Waves in Condensed Matter - 1983*, edited by J. R. Asay *et al.*, (Elsevier, Amsterdam, 1984), pp. 91–94.
[5] D. Santamaria-Perez *et al.*, J. Chem. Phys. **130**, 124509 (2009).
[6] R. S. Hixson *et al.*, Phys. Rev. Lett. **62**, 637 (1989).
[7] A. B. Belonoshko *et al.*, Phys. Rev. Lett. **100**, 135701 (2008), and references therein.
[8] A. S. Mikhaylushkin *et al.*, Phys. Rev. Lett. **101**, 049602 (2008).
[9] J. Zhang and Y. Zhao, Nature (London) **430**, 332 (2004).
[10] J. Zhang and Y. Zhao, Nature (London) **437**, 1057 (2005).
[11] M. Ross, D. Errandonea, and R. Boehler, Phys. Rev. B **76**, 184118 (2007).
[12] C. J. Wu *et al.*, Nature Mater. **8**, 223 (2009).
[13] J. A. Moriarty *et al.*, J. Mater. Res. **21**, 563 (2006).
[14] D. Orlikowski, P. Söderlind, and J. A. Moriarty, Phys. Rev. B **74**, 054109 (2006).
[15] F. H. Streitz and J. A. Moriarty, LLNL Report No. UCRL-JCPS-134455, 2002; F. H. Streitz, J. N. Glosli, and M. V. Patel, Phys. Rev. Lett. **96**, 225701 (2006).
[16] P. E. Blöchl, Phys. Rev. B **50**, 17 953 (1994); G. Kresse and D. Joubert, Phys. Rev. B **59**, 1758 (1999).
[17] G. Kresse and J. Hafner, Phys. Rev. B **48**, 13115 (1993); G. Kresse and J. Furthmüller, Comput. Mater. Sci. **6**, 15 (1996).
[18] In the present work the small displacement method was used, see D. Alfé, Comput. Phys. Commun. **180**, 2622 (2009); see also http://chianti.geol.ucl.ac.uk/~dario.
[19] Y. Wang and J. P. Perdew, Phys. Rev. B **44**, 13298 (1991); J. P. Perdew *et al.*, Phys. Rev. B **46**, 6671 (1992).
[20] H. J. Monkhorst and J. D. Pack, Phys. Rev. B **13**, 5188 (1976).
[21] M. Methfessel and A. T. Paxton, Phys. Rev. B **40**, 3616 (1989).
[22] P. E. Blöchl, O. Jepsen, and O. K. Andersen, Phys. Rev. B **49**, 16 223 (1994).
[23] A. B. Belonoshko *et al.*, Phys. Rev. B **73**, 012201 (2006).
[24] S. Taioli *et al.*, Phys. Rev. B **75**, 214103 (2007).
[25] R. Hixson (private communication).
[26] J. R. Asay, L. C. Chhabildas, G. I. Kerley, and T. G. Trucano, in *Shock Waves in Condensed Matter*, edited by Y. M. Gupta (Plenum, New York, 1986), pp. 145–149.
[27] Y.-Y. Yu *et al.*, Baozha Yu Chongji (Explosion and Shock Waves) **26**, 486 (2006).
[28] J. Emsley, *The Elements* (Oxford University Press, New York, 1999), 3rd ed., p. 200.
[29] L. L. Hsiung and D. H. Lassila, Scr. Mater. **38**, 1371 (1998); **39**, 603 (1998); Acta Mater. **48**, 4851 (2000).
[30] H. Cynn and C.-S. Yoo, Phys. Rev. B **59**, 8526 (1999).
[31] J. Eggert *et al.*, AIP Conf. Proc. **955**, 1177 (2007).